

THE SYSTEM 1,2,4,5-TETRACHLOROBENZENE + 1,2,4,5-TETRABROMOBENZENE.

Part 1. Experimental phase diagram (93–460 K)

D. MONDIEIG, J.R. HOUSTY and Y. HAGET

*Laboratoire de Cristallographie et de Physique Cristalline, U.R.A. 144 au CNRS,
Université Bordeaux I (France)*

M.A. CUEVAS-DIARTE

Departament de Cristallografia, Universitat de Barcelona (Spain)

H.A.J. OONK

Chemical Thermodynamics Group, Utrecht University (The Netherlands)

(Received 1 June 1990)

ABSTRACT

Equilibrium relations in the system 1,2,4,5-tetrachlorobenzene + 1,2,4,5-tetrabromobenzene have been studied from 93 to 460 K by means of X-ray crystallography and thermal analytical methods. The result is an experimental $T-x$ phase diagram with three three-phase equilibria (one of the peritectic and two of the eutectoid type), seven two-phase regions and four single-phase fields corresponding to mixed crystalline solids.

INTRODUCTION

The work reported here is part of the research program of the Réseau Européen sur les alliages Moléculaires (REALM), the organization in which our research groups participate. The research carried out by REALM bears upon the miscibility of organic substances and the properties of their mixed crystals (molecular alloys). Several systems composed of di- and tri-R substituted benzenes with $R = \text{Br}, \text{Cl}, \text{CH}_3$ have already been studied [1–6]. The work reported here concerns the experimental determination of the phase diagram of 1,2,4,5-tetrachlorobenzene–1,2,4,5-tetrabromobenzene (TeCB–TeBB). Both substances show polymorphism [7,8] of which we will recall the essentials. To our knowledge, the only work on TeCB–TeBB is the determination of the solid–liquid phase diagram by Rheinboldt et al. [9], who reported a single solid–liquid loop and complete subsolidus miscibility. The phase diagram reported here is considerably more complicated.

EXPERIMENTAL

Starting materials

TeCB was purchased from Aldrich and TeBB from Eastman Kodak; their purities were 99.6 and 98%, respectively, as shown by mass spectrometry in combination with gas chromatography. The commercial TeBB was purified to 99.8%; the commercial TeCB was used without further purification.

Sample preparation

Samples were prepared by crystallization from a solution in diethylether RP. Weighed amounts of the two substances were dissolved in ether, after which the solvent was evaporated under a gentle stream of nitrogen.

Methods of analysis

The phase diagram was determined by means of two complementary types of technique, corresponding to isoplethic and isothermal measurements, respectively. The isothermal measurements, consisting of X-ray diffractometry, were carried out at 293 K for all the selected concentrations. The polycrystalline samples were studied by $\text{Cu } K\alpha$ radiation, using internal calibration and making corrections for $K\alpha_1 K\alpha_2$ splitting. The isoplethic measurements were realized by two methods of thermal analysis.

(i) Diffractometric analysis using a Guinier–Lenné (GL) or a Guinier–Simon (GS) camera, in which the sample is subjected to a temperature variation program. From the crystallographic behaviour of the sample as a function of temperature the stability ranges of the various phases can be derived.

(ii) Differential thermal analysis (DTA), which permits the determination of the (solid–solid and solid–liquid) transition temperatures as well as the corresponding enthalpy effects. The interpretation of the signals was made by our shape-factors method [10,11]. The results were treated by a statistical method: several (at least five) independent measurements were made and subjected to Student's formula at the 95% confidence level.

For each type of measurement several precautions were taken to prevent preferential sublimation of the sample (sealed capsules and/or tubes; protecting chamber for long X-ray exposures); details can be found in ref. 7.

POLYMORPHISM

Details of the polymorphic nature of the two substances can be found in ref. 8. In this section we just give the elements necessary for reading this paper.

TABLE 1
Polymorphism of the pure components

| Compound | Form | T (K) | a (Å) | b (Å) | c (Å) | β (deg) | Ref. |
|----------|----------|------------|--------------------|--------------------|-------------------|-------------------|------|
| TeCB | β | 293 | 9.720 ± 0.010 | 10.625 ± 0.012 | 3.858 ± 0.007 | 103.37 ± 0.09 | 7, 8 |
| TeBB | β | 293 | 10.313 ± 0.010 | 10.712 ± 0.012 | 4.016 ± 0.006 | 102.50 ± 0.06 | 7, 8 |
| | γ | 332 | 10.00 ± 0.01 | 11.18 ± 0.01 | 4.07 ± 0.02 | 103.80 ± 0.83 | 13 |

Tetrachlorobenzene

TeCB occurs in two crystalline forms: the α form at low temperatures and the β form above 185.6 ± 3.3 K. The enthalpy of transition has a low value (95 ± 25 J mol⁻¹). The α form is triclinic ($P\bar{1}$, $Z = 2$). According to Herbstein [12] the cell dimensions at 150 K are the following: $a = 9.60$ Å, $b = 10.59$ Å, $c = 3.76$ Å, $\alpha = 95^\circ$, $\beta = 102.5^\circ$, $\gamma = 92.5^\circ$. The β form is monoclinic ($P2_1/a$, $Z = 2$); its cell dimensions are given in Table 1. The melting point of the β form is 412.8 ± 0.3 K and the enthalpy of melting $26\,340 \pm 500$ J mol⁻¹.

Tetrabromobenzene

TeBB presents two crystalline forms, both monoclinic ($P2_1/a$, $Z = 2$). One is stable at room temperature, the other being stable above 306.8 ± 0.5 K ($\Delta H = 335 \pm 45$ J mol⁻¹). To refer to these forms, we shall use the notation adopted by Gafner and Herbstein [13]: the form which is stable at ambient temperature is named β , in conformity with the β form of TeCB. The same authors state that TeCB and TeBB are isomorphous at ambient temperature. The other form is named γ ; its unit-cell dimensions are given in Table 1; its melting point is 453.1 ± 0.4 K, with $\Delta H = 27\,880 \pm 590$ J mol⁻¹.

ISOTHERMAL STUDY AT 293 K

The course of diffraction lines as a function of composition

The results that are presented here are in the main from diffractometric studies carried out at 293 K; they are in agreement with the results obtained by the isoplethic methods, which are presented later.

We studied the course of the set of diffraction lines as a function of composition. We took samples at 0.1 intervals of the composition variable x ,

which is the mole fraction of TeBB. In order to illustrate this, take the line (210); its variation with x is shown in Fig. 1. We observe the following points.

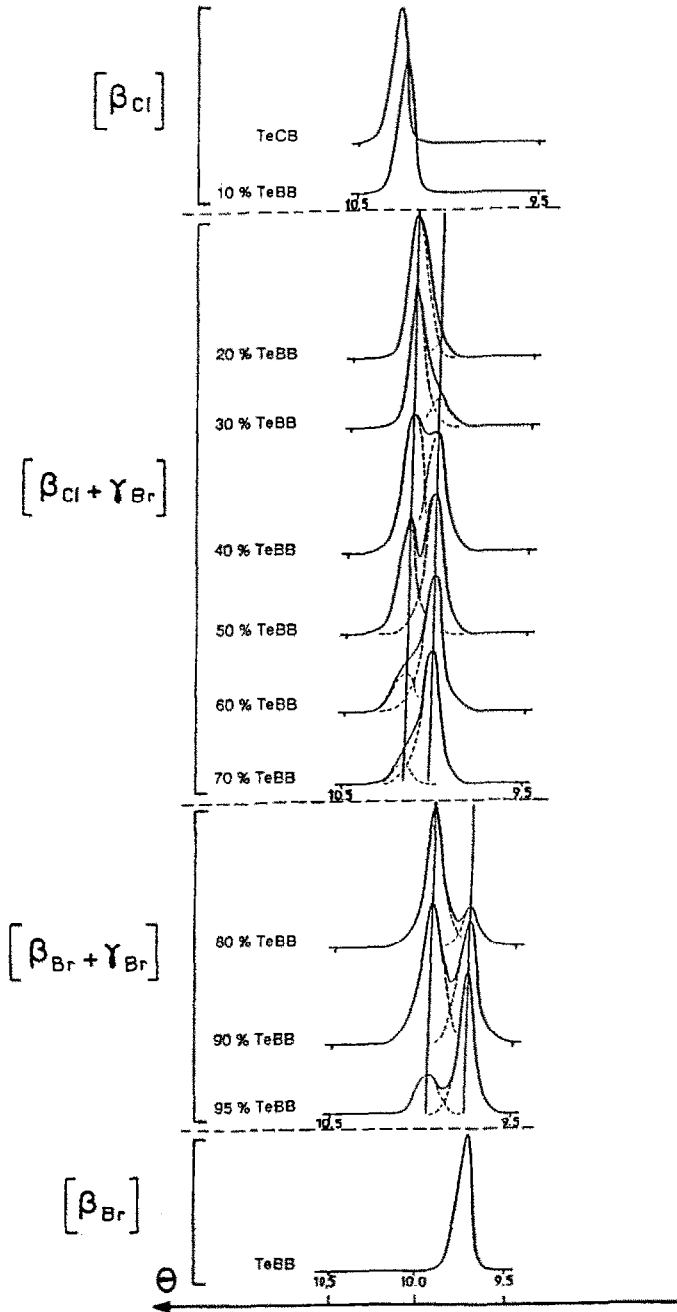


Fig. 1. Variation of the intensity and position of the (210) reflection as a function of composition.

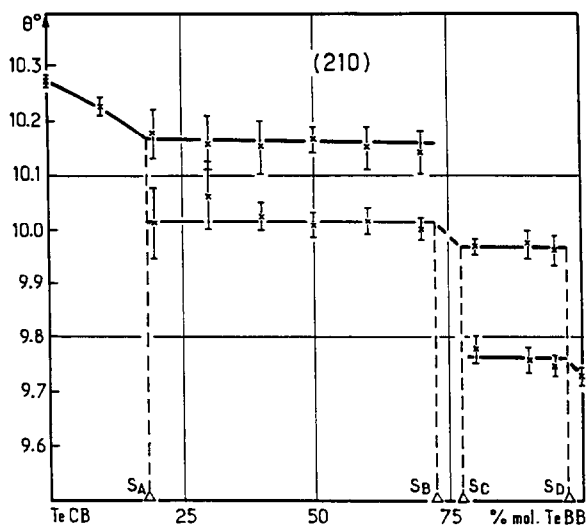


Fig. 2. Variation of the position of the (210) reflection as a function of composition.

(i) For small values of x (e.g., sample with $x = 0.1$) there is just a displacement of the peaks towards smaller angles (compared with pure TeCB); the peaks do not broaden and there is no splitting of rays: one is dealing with the formation of a typical molecular alloy. There is syncrystallization and the introduction of TeBB molecules in the β -type lattice causes an increase in the distances between the lattice planes.

(ii) For samples with $x = 0.2$ or more, there is a splitting of the peaks, which is evidence for a two-phase region. However, a close examination of the course of the whole set of peaks as a function of x shows that two such two-phase regions make their appearance: a region from S_A to S_B , and another from S_C to S_D .

To proceed further we made deconvolutions of the various diffraction lines. These deconvolutions are shown in Fig. 1 for the line (210) by means of dashed curves. It follows that in the two composition zones, the positions of the two doubled peaks, within the limits of uncertainty, can be considered as being constant. Moreover, the intensities of deconvoluted peaks change with the composition. One of the peaks diminishes in intensity with increasing x , whereas the other becomes progressively more pronounced. This behaviour is typical of a two-phase region.

An analysis of the changes of the various peaks enabled us to determine the nature and composition of the limiting phases of the phase regions. As a result, at 293 K one can distinguish, as a function of x , the following five successive fields (Fig. 2 and Table 2: (i) a single-phase field of β_{Cl} type going from pure TeCB to mixed crystal ($S_A = \text{TeCB}_{0.82}\text{TeBB}_{0.18}$); (ii) a two-phase field [$\beta_{Cl} + \gamma_{Br}$] where S_A and S_B coexist ($S_B = \text{TeCB}_{0.28}\text{TeBB}_{0.72}$); (iii) a very narrow single phase field of type γ_{Br} , extending from S_B to S_C with

TABLE 2

Limiting solid solutions for the various types

| Solution | Type | x^a |
|----------|-----------------|-------|
| S_A | $[\beta_{Cl}]$ | 0.18 |
| S_B | $[\gamma_{Br}]$ | 0.72 |
| S_C | $[\gamma_{Br}]$ | 0.77 |
| S_D | $[\beta_{Br}]$ | 0.97 |

^a Mole fraction TeBB.

$S_C = \text{TeCB}_{0.23}\text{TeBB}_{0.77}$; (iv) a two-phase field $[\gamma_{Br} + \beta_{Br}]$ where S_C and S_D coexist with $S_D = \text{TeCB}_{0.03}\text{TeBB}_{0.97}$; and finally, (v) a very narrow single-phase field of β_{Br} type, extending from $x = 0.97$ to $x = 1.00$, i.e. to pure TeBB).

Crystallographic characterization of the alloys at 293 K

With the help of diffractograms, we calculated, by least-squares refinement, the unit-cell dimensions of the various mixed crystals. The calculated values are given in Table 3.

STUDY AS A FUNCTION OF TEMPERATURE

To start with, we shall examine for a given value of x the principal characteristics of the course of diffraction lines as a function of temperature. The results obtained for $x = 0.50$ are particularly revealing. Thereafter we shall analyze the effect of the polymorphism of TeCB and then the polymorphism of TeBB. Finally after having established the limits of miscibility between β_{Cl} and β_{Br} and between β_{Cl} and γ_{Br} , we shall study the solid \rightarrow liquid transition.

Exploring analysis of the sample with $x = 0.50$

In Fig. 3(a), the GS and GL photographs are shown; they were obtained with increasing temperature, from 93 to 293 K and from 293 to 473 K. In addition, Fig. 3(b) is a schematic reproduction of one of the most revealing parts of the photographs; that which shows the evolution of the lines (120) and (210). Examination of these photographs gives rise to the following six successive distinct fields.

(i) From 93 K (the lower limit of our study) to 213 K there are two families of "coexisting" lines, one of the type β_{Br} and the other β_{Cl} ; one is dealing with a two-phase region, the $[\beta_{Cl} + \beta_{Br}]$ region.

(ii) From 213 to 383 K there are again two families of coexisting lines. One of these still belongs to β_{Cl} . The other family shows the appearance of γ_{Br} . One is in the $[\beta_{Cl} + \gamma_{Br}]$ two-phase region.

TABLE 3
Crystallographic characterization of the various alloys

| Name | $x(\text{TeBB})$ | Type | a (Å) | b (Å) | c (Å) | β (deg) | V (Å ³) |
|-------|------------------|----------------------|--------------------|--------------------|-------------------|-------------------|-----------------------|
| TeCB | 0.00 | β_{Cl} | 9.720 ± 0.010 | 10.625 ± 0.012 | 3.858 ± 0.007 | 103.37 ± 0.09 | 387.6 ± 0.7 |
| | 0.10 | β_{Cl} | 9.758 ± 0.010 | 10.665 ± 0.013 | 3.877 ± 0.005 | 103.69 ± 0.08 | 392.7 ± 0.8 |
| | 0.18 | β_{Cl} | 9.813 ± 0.013 | 10.703 ± 0.012 | 3.866 ± 0.009 | 103.86 ± 0.15 | 394.0 ± 0.5 |
| S_B | 0.72 | γ_{Br} | 9.971 ± 0.010 | 10.969 ± 0.018 | 4.017 ± 0.006 | 103.08 ± 0.11 | 427.9 ± 0.9 |
| | 0.77 | γ_{Br} | 9.970 ± 0.014 | 10.978 ± 0.014 | 4.020 ± 0.007 | 103.00 ± 0.12 | 428.7 ± 0.9 |
| S_D | 0.97 | β_{Br} | 10.286 ± 0.013 | 10.710 ± 0.011 | 4.019 ± 0.010 | 102.10 ± 0.16 | 433.0 ± 0.9 |
| | 1.00 | β_{Br} | 10.314 ± 0.010 | 10.710 ± 0.012 | 4.016 ± 0.006 | 102.50 ± 0.06 | 433.2 ± 0.9 |

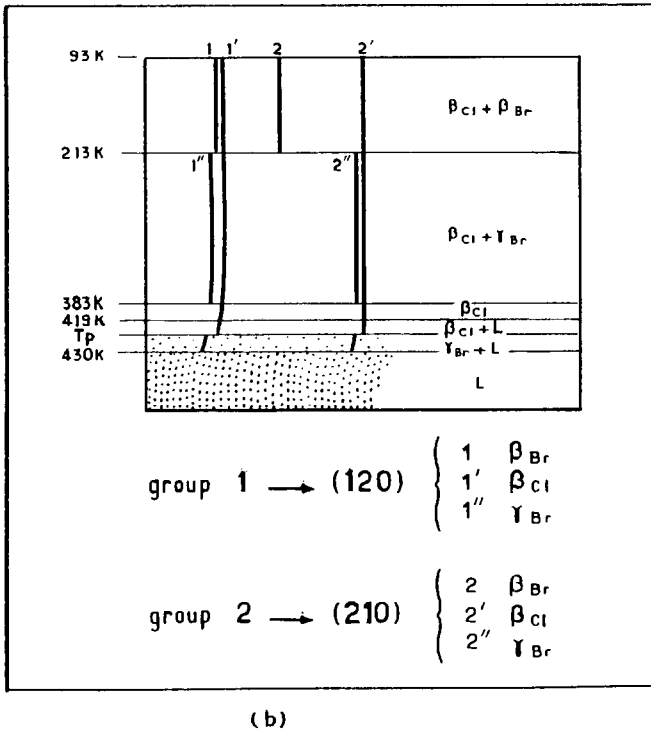
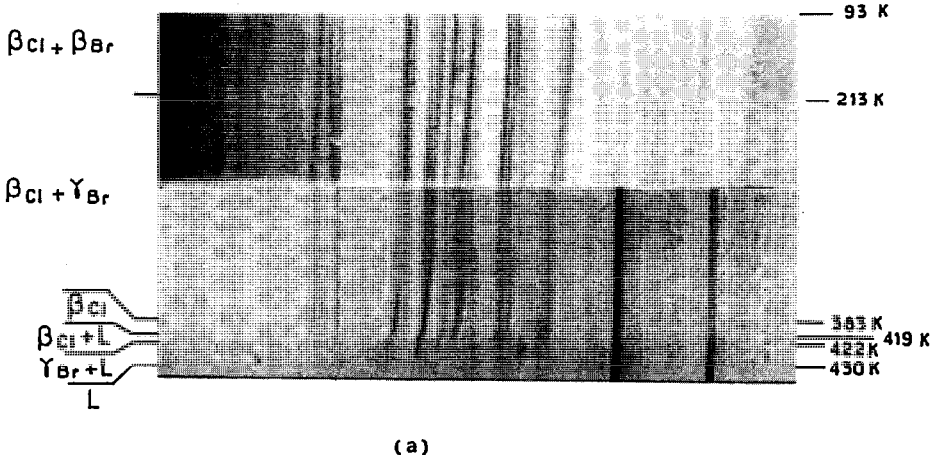


Fig. 3. Sample with composition $x = 0.50$: (a) GL and GS photographs; (b) evolution of the (120) and (210) reflections as a function of temperature.

(iii) From 383 to 419 K the family of lines corresponding to γ_{Br} are no longer present. One is dealing with a single-phase field, the $[\beta_{Cl}]$ field.

(iv) From 419 K a continuous background makes its appearance: the sample starts to melt. Up to 423 K there are still the β_{Cl} lines. One is in the solid-liquid two-phase region, $[\beta_{Cl} + L]$.

(v) At 423 K the β_{Cl} lines are replaced by a family of lines which was observed before: the γ_{Br} family. One is in the $[\gamma_{Br} + L]$ two-phase region, up to 433 K.

(vi) Above 433 K, all diffraction lines have disappeared, the background is more pronounced: one is in the liquid single-phase field.

At this moment one can draw the following conclusions:

(i) The β_{Cl} and γ_{Br} forms are not miscible in all proportions.

(ii) The existence of the $[\beta_{Cl} + \beta_{Br}]$ two-phase region shows that the β_{Cl} and β_{Br} forms are not completely miscible either.

(iii) The transition from the two-phase region $[\beta_{Cl} + \beta_{Br}]$ to the other, $[\beta_{Cl} + \gamma_{Br}]$, shows that at about 223 K there is an invariant three-phase equilibrium; it is of a eutectoid type, as it is lower than the $\beta \rightarrow \gamma$ transition temperature of TeBB.

(iv) The $[\beta_{Cl}]$ single-phase field becomes broader at higher temperature. At 293 K it is from $x = 0.00$ to $x = 0.18$, while at 419 K it is already beyond $x = 0.50$.

(v) The sequence of the two-phase regions $[\beta_{Cl} + L]$ and $[\gamma_{Br} + L]$ implies that the melting is of the peritectic type, the peritectic three-phase equilibrium being in the vicinity of 423 K,

Consequences of the polymorphism of TeCB

With increasing temperature pure TeCB changes from α to β at 185.6 K. Although the transition is first-order, the accompanying heat effect is very weak, which implies that the change should preferably be studied by X-ray diffraction. This is particularly true for the samples with $x = 0.05$, of which the GS photograph is given in Fig. 4. A close examination of the latter reveals the following three distinct successive parts.

(i) A part from 93 to about 103 K where only α_{Cl} lines are observed.

(ii) Another part, from about 153 K to the melting of the sample, with another single family of lines; the single-phase field $[\beta_{Cl}]$ is observed.

(iii) Between the two preceding parts, from 103 to 293 K, there is a part with two families of lines. One is dealing with the two-phase region $[\alpha_{Cl} +$



Fig. 4. GS photograph for the sample with composition $x = 0.05$.

β_{Cl}]. The introduction of TeBB in the lattice of TeCB lowers the $\alpha \rightarrow \beta$ transition temperature.

The study of the sample with $x = 0.10$ revealed that at 93 K one is already in the field $[\beta_{Cl} + \beta_{Br}]$. As a consequence, at low temperatures ($T < 150$ K) the $[\beta_{Cl}]$ single-phase field is extremely narrow; a small zone between $x = 0.05$ and 0.10.

Incidentally, we never observed the transition between the two two-phase regions, $[\alpha_{Cl} + \beta_{Cl}]$ to $[\beta_{Cl} + \beta_{Br}]$. Apparently, the eutectoid three-phase equilibrium is below 93 K.

Consequences of the polymorphism of TeBB

On increasing the temperature TeBB changes from the β to γ form at 306.8 K with a relatively weak heat effect. At 293 K this polymorphism manifests itself in the isothermal section of the phase diagram through the $[\gamma_{Br} + \beta_{Br}]$ two-phase region, corresponding with a solid–solid loop. The limits of the latter at 293 K have already been established (Table 2).

The upper limit of the $[\gamma_{Br} + \beta_{Br}]$ loop

The high-temperature limits of the solid–solid loop, $[\gamma_{Br} + \beta_{Br}]$, could be determined using a GS camera on samples with $x = 0.80, 0.90$ and 0.95. As an example, the GS photograph in Fig. 5 clearly shows the transition from a part with two families of lines $\gamma_{Br} + \beta_{Br}$ to a part with one remaining family of lines, i.e. that corresponding to γ_{Br} .

Inspection of the GL photographs of the sample with $x = 0.70$ (Fig. 6) reveals the presence of the transition at about 218 K from one solid–solid two-phase region to another: $[\beta_{Cl} + \beta_{Br}] \rightarrow [\gamma_{Br} + \beta_{Br}]$. It means that the eutectoid line extends beyond $x = 0.70$. In addition it follows that the two fields $[\beta_{Cl} + \beta_{Br}]$ and $[\gamma_{Br} + \beta_{Br}]$ are not far away from one another.

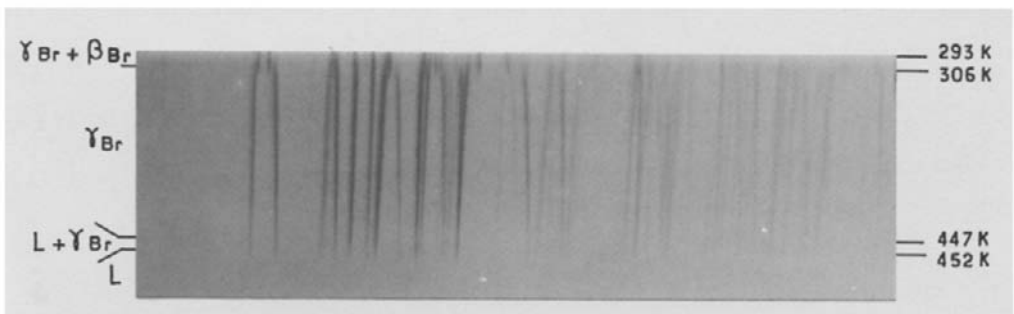
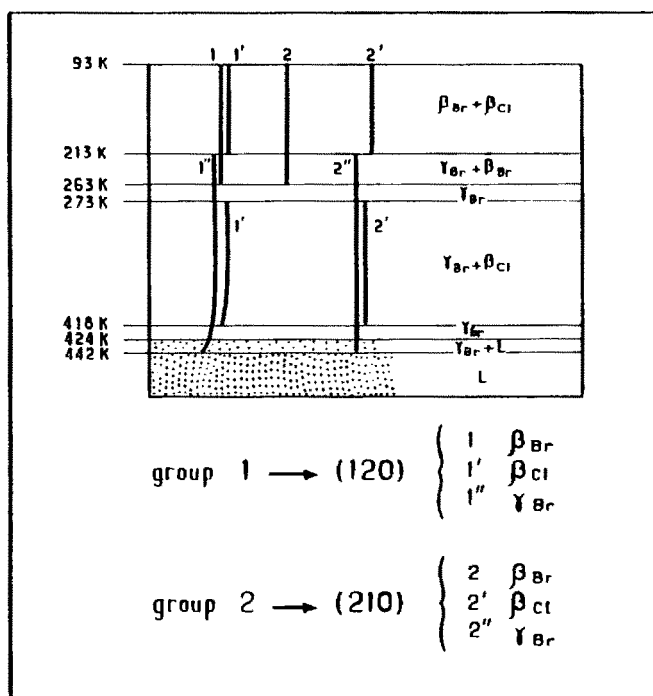
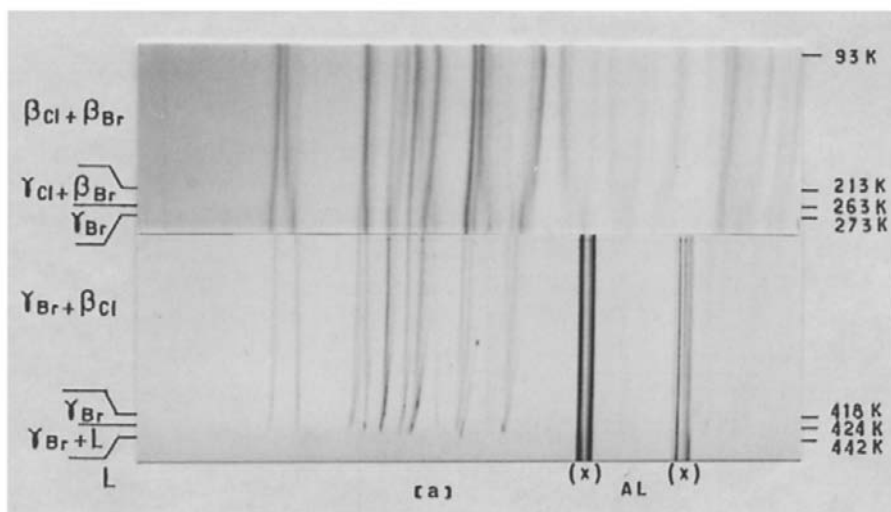


Fig. 5. GS photograph for the sample with composition $x = 0.95$.

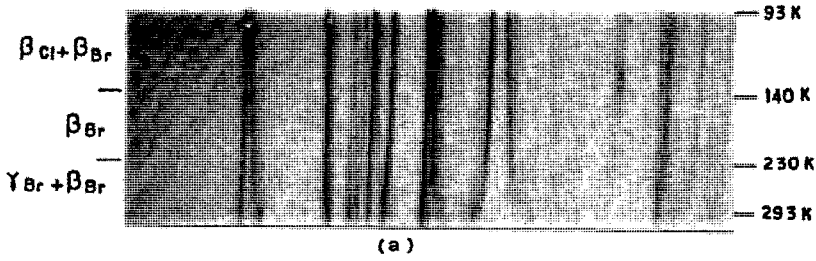


(b)

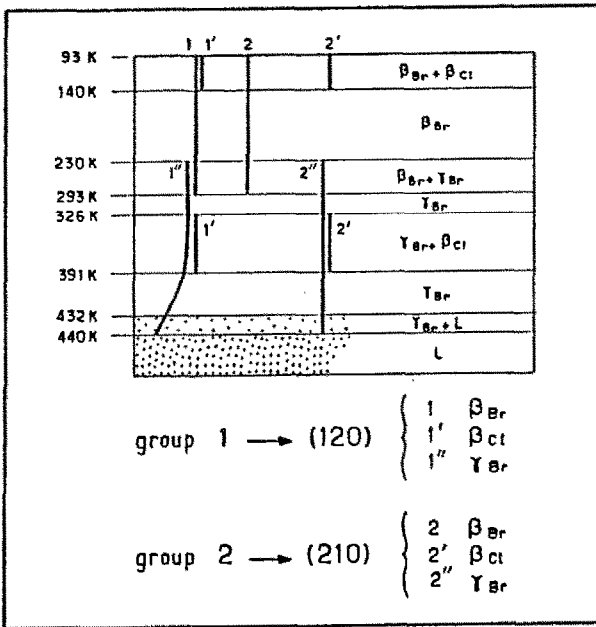
Fig. 6. Sample with composition $x = 0.70$; (a) GL and GS photographs; (b) evolution of the (120) and (210) reflections as a function of temperature.

The lower limit of the $[\gamma_{Br} + \beta_{Br}]$ loop

The GS photograph, (Fig. 7a, b, for $x = 0.80$) reveals that, on increasing the temperature from 93 to 293 K, there are three successive domains: to



(a)



(b)

Fig. 7. Sample with composition $x = 0.80$: (a) GS photograph; (b) evolution of the (120) and (210) reflections as a function of temperature.

about 143 K, the $[\beta_{Cl} + \beta_{Br}]$ two-phase region; from 143 to 230 K, the β_{Br} single-phase field; above 230 K, the $[\gamma_{Br} + \beta_{Br}]$ two-phase region.

As a result, the lower limit of the $[\gamma_{Br} + \beta_{Br}]$ loop for $x = 0.80$ will be about 230 K.

Extent of the solid single-phase fields and positions of three-phase equilibrium lines

Limits of miscibility in the α_{Cl} form

The field where molecular alloys of the α_{Cl} type are found is rather narrow. At 93 K, it goes up to about 6% of TeBB.

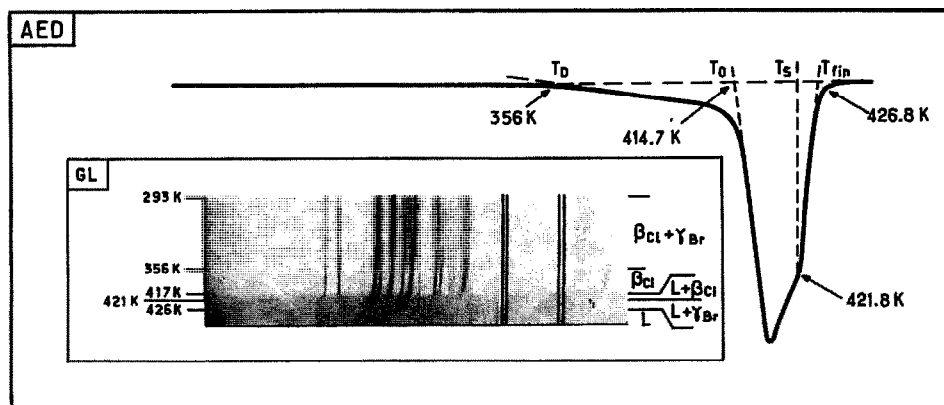


Fig. 8. DTA curve and GL photograph for $x = 0.40$.

The eutectoid $M''E''N''$

The eutectoid temperature is below 93 K; in the final diagram, Fig. 11, it is indicated by dashed lines.

The $[\beta_{Cl}]$ and $[\beta_{Br}]$ fields below the eutectoid ($M'E'N'$) temperature

$x = 0.10$ corresponds to a location in the $[\beta_{Cl} + \beta_{Br}]$ two-phase field, irrespective of temperature. For $x = 0.05$ and $T > 153$ K one is in the $[\beta_{Cl}]$ single-phase field. For these reasons, the left-hand boundary of the $[\beta_{Cl} + \beta_{Br}]$ two-phase region was drawn as shown in Fig. 11.

We know that at 143 K the right-hand boundary of the $[\beta_{Cl} + \beta_{Br}]$ two-phase region is near $x = 0.80$. Furthermore, it follows, from our analyses, that the single-phase field of the molecular alloys of β_{Br} type reaches its minimum width at the eutectoid temperature.

The eutectoid $M'E'N'$

The results of the isoplethic thermal and X-ray analysis of the set of samples from $x = 0.10$ up to $x = 0.70$ allowed us to establish the characteristics of the eutectoid $M'E'N'$. Its temperature is 213 ± 15 K and its range on the mole-fraction scale is from 0.08 to 0.75, the position of E' being at about 0.60.

The $[\beta_{Cl}]$ and $[\gamma_{Br}]$ fields above the eutectoid ($M'E'N'$) temperature

The isothermal study at 293 K has already revealed that the single-phase field of the alloys of β_{Cl} type extends to $x = 0.18$. Going to lower temperatures, the boundary of $[\beta_{Cl}]$ moves towards lower x values. This is shown by the results obtained for the sample with $x = 0.10$, for which the boundary between $[\beta_{Cl}]$ and $[\beta_{Cl} + \gamma_{Br}]$ is at about 261 K. On the other hand, for

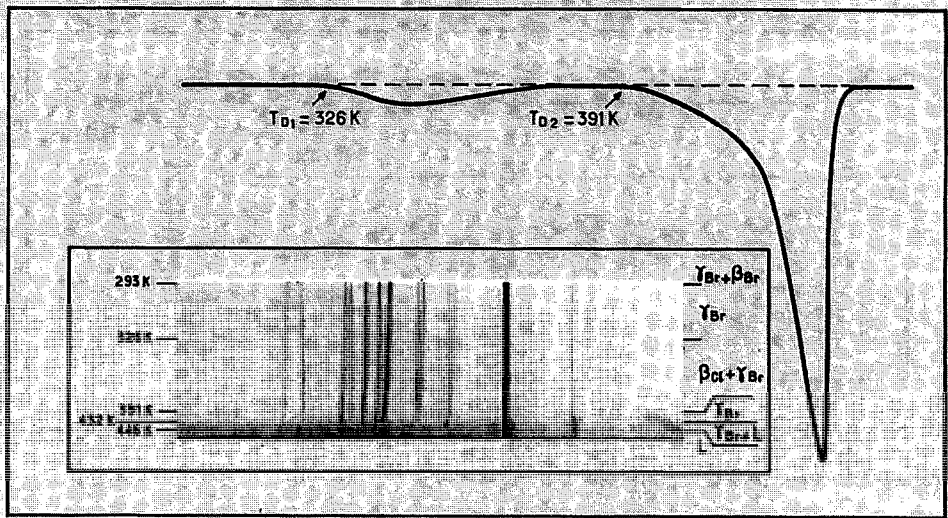


Fig. 9. DTA curve and GL photograph for $x = 0.80$.

$T > 293$ K the $[\beta_{Cl}]$ field becomes broader. This phenomenon can be discerned and analyzed by means of GL photographs as well as by thermal analyses on samples from $x = 0.20$ to 0.60 . As an example, Fig. 8 shows the results obtained by the two techniques for $x = 0.40$. The thermal analysis signals show a deviation from the base line prior to the fusion peak (on increasing x the distance from T_D to the fusion peak decreases). This take-off is an indication for the transition from the $[\beta_{Cl} + \gamma_{Br}]$ two-phase region to the $[\beta_{Cl}]$ single-phase region. It is confirmed by the GL experiments where the two families of lines corresponding to $\beta_{Cl} + \gamma_{Br}$ change into a pattern that corresponds to one family of β_{Cl} lines. At high temperature, the single-phase field corresponding to the formation of alloys of the β_{Cl} form can reach a content of 60% TeBB.

Regarding the formation of alloys of the γ_{Br} form, the experiments on the samples with $x = 0.70$ and 0.80 give evidence for an interesting (because it is rare) phenomenon, namely that of the retrograde course of an equilibrium line in a $T-x$ phase diagram. Inspection of the output of the analyses (Fig. 9), on the sample with $x = 0.80$ gives rise to the following observations:

(i) Regarding the GL photographs. At about 326 K there is a transition from a pattern with one family of lines, γ_{Br} , to a pattern with two families of lines, $\beta_{Cl} + \gamma_{Br}$. The intensity of the β_{Cl} family is weak, meaning that the boundary between $[\beta_{Cl} + \gamma_{Br}]$ and $[\gamma_{Br}]$ is close to $x = 0.80$. At about 391 K the β_{Cl} lines disappear, implying a transition from $[\gamma_{Br} + \beta_{Cl}]$ to $[\gamma_{Br}]$.

(ii) Regarding the DTA curves. At 326 K there is a take-off from the base line which extends with temperature; this is evidence for a transition, implying solid-solid diffusion. At 391 K there is another take-off from the

base line, which again is evidence for a transition which implies solid–state diffusion, taking place before melting.

The results obtained by GL and by DTA are mutually in agreement. They give rise to the observation that for $x = 0.80$ (it is also true for $x = 0.70$, but the effect is somewhat less pronounced) on increasing temperature there is a succession of fields $[\gamma_{Br}] \rightarrow [\beta_{Cl} + \gamma_{Br}] \rightarrow [\gamma_{Br}]$. One is dealing with a “re-entry” phenomenon, also referred to as “retrograde”. It follows that the γ_{Br} single-phase field shows a change of its extent of 0.22 on the mole fraction scale for 306 K to just 0.175 at about 353 K, after which it again increases to a maximum value of 0.31 at the peritectic temperature.

The solid–liquid equilibria

The determination of different solid–liquid equilibria was carried out by the combined use of thermal analysis and X-ray diffraction (GL, GS). The nature of the solid phases was found by GL, while the temperatures involved could be precisely determined by DTA. The DTA curves obtained for the various compositions are shown in Fig. 10. The DTA curves were analyzed by means of the shape-factors method which we published recently [10,11]. Results are given in Table 4. We just give here the characteristics of the peritectic K, M, N: $T_p = 422.2 \pm 0.9$ K, $x_K = 0.36$, $x_M = 0.62$ and $x_N = 0.68$.

TABLE 4
Solid–liquid transition as a function of composition ^a

| Mole fractions $x(\text{TeBB})$ | Solidus $T_{\text{sol}} \text{ (K)}$ | Peritectic $T_{\text{per}} \text{ (K)}$ | Liquidus $T_{\text{liq}} \text{ (K)}$ |
|------------------------------------|---|--|--|
| TeCB | 412.8 ± 0.3 | | |
| 0.05 | 412.5 ± 1.4 | | 413.6 ± 0.5 |
| 0.10 | 412.4 ± 1.3 | | 413.4 ± 0.6 |
| 0.20 | 413.6 ± 1.2 | | 415.1 ± 0.5 |
| 0.30 | 413.3 ± 1.4 | | 420.4 ± 1.3 |
| 0.40 | 414.7 ± 1.5 | 421.2 ± 2.0 | 425.5 ± 2.4 |
| 0.50 | 419.1 ± 1.0 | 421.7 ± 1.0 | 430.4 ± 0.7 |
| 0.60 | 419.6 ± 1.5 | 421.9 ± 1.3 | 437.2 ± 2.0 |
| 0.65 | | 422.7 ± 1.5 | 440.6 ± 1.1 |
| 0.70 | 424.0 ± 2.0 | | 441.7 ± 1.3 |
| 0.80 | 431.9 ± 2.0 | | 445.8 ± 0.8 |
| 0.90 | 441.7 ± 1.5 | | 449.3 ± 1.3 |
| 0.95 | 446.5 ± 1.5 | | 451.6 ± 0.7 |
| TeBB | 453.1 ± 0.4 | | |

^a Note that the results have greater precision than those obtained for solid–solid transitions, due to the fact that the phenomena do not entirely take place in a solid environment and, in addition, involve more energy.

CONCLUSIONS

The polymorphism of the components of this system give rise to the "rich" diagram which is shown in Fig. 11; rich because there are three invariant equilibria: a peritectic equilibrium at 422.2 ± 0.9 K and two equilibria of the eutectoid type, one at 213 ± 15 K and the other below 93 K. There are twelve different regions in the $T-x$ diagram. It may be emphasized that it is the variety of experimental techniques employed (isothermal X-ray experiments at 293 K and isoplethic DTA and GL or GS photography

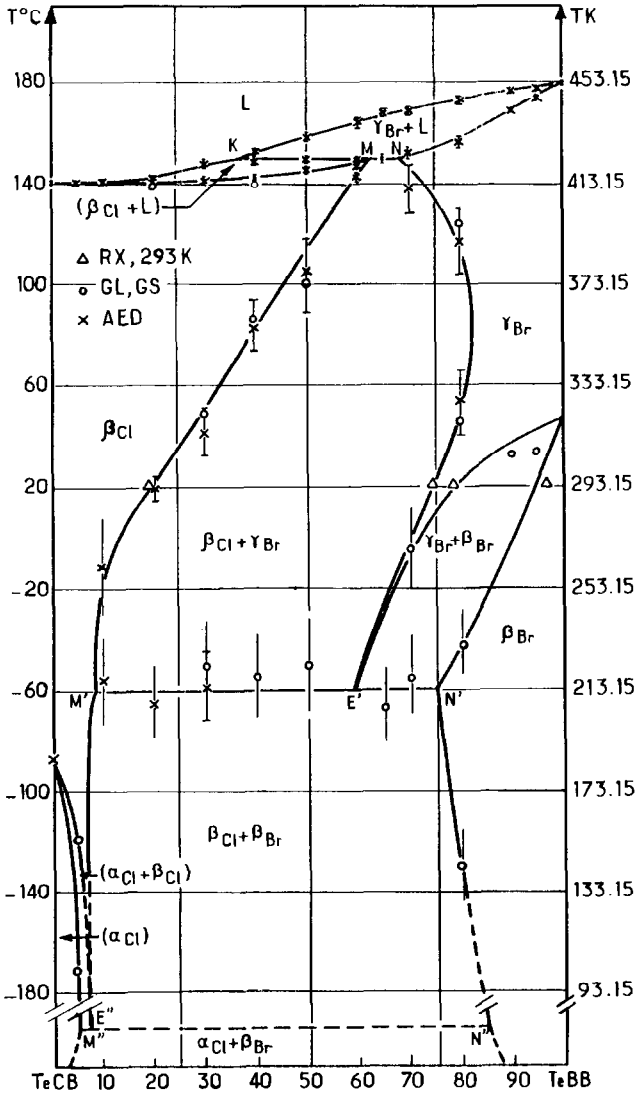


Fig. 11. Experimental phase diagram of the system TeCB-TeBB from 93 to 473 K.

that has enabled the various phases and their limits of stability to be determined.

The twelve regions involve the liquid field, two solid–liquid two-phase regions, five solid–solid two-phase regions and four single-phase fields corresponding to molecular alloys.

The four single-phase fields are (i) a field of α_{Cl} type which is found below 185.6 K for compositions close to pure TeCB; (ii) a field of β_{Br} type characterised by a high TeBB content, which is at any rate below 306.8 K and its maximum extent is 0.25 on the mole fraction scale at 213 K; (iii) a field of β_{Cl} type, which is by far the greatest molecular alloy single-phase field as it can reach an x value of 0.60; (iv) a field of γ_{Br} type which shows retrograde behaviour, its width changing from 0.22 at 306 K to 0.175 at about 353 K after which it increases to its maximum width of 0.31 at 422.2 K, the peritectic temperature.

In the context of the rules that govern the formation of mixed crystals, the present system poses an interesting problem. Although we have used the notations β (β_{Cl} and β_{Br}) and γ (γ_{Br}), which were given by the authors who first described the forms, we should ask ourselves for which combination the structural resemblances are the most pronounced. Is it between β_{Cl} and β_{Br} or is it between β_{Cl} and γ_{Br} ? And for which combination one should speak of isomorphism? We intend to return to this problem in a forthcoming paper (Part II) which will deal with a thermodynamic phase-diagram analysis of this very peculiar system.

REFERENCES

- 1 Y. Haget, J.R. Housty, A. Maïga, L. Bonpunt, N.B. Chanh, M.A. Cuevas-Diarte and E. Estop, *J. Chim. Phys.*, 81(3) (1984) 197.
- 2 M. Bennouni, A. Belaaraj, R. Courchinoux, J.R. Housty, N.B. Chanh, Y. Haget, X. Alcobé, M.A. Cuevas-Diarte and H.A.J. Oonk, in J.J. Counieux and M.T. Saugier Cohen-Adad (eds.), *Les équilibres entre phases*, Vol. 13, Lyon, 1987, p. 205.
- 3 M. Labrador, T. Calvet, E. Tauler, M.A. Cuevas-Diarte, E. Estop and Y. Haget, *J. Chim. Phys.*, 84 (7–8) (1987) 95.
- 4 X. Alcobé, E. Estop, E. Tauler, M. Labrador, M.A. Cuevas-Diarte and Y. Haget, *Mater. Res. Bull.*, 23 (1988) 177.
- 5 H.A.J. Oonk, T. Calvet, M.A. Cuevas-Diarte, Y. Haget, J.C. van Miltenburg and E.H. Tenissen, *Thermochim. Acta*, 146 (1989) 297.
- 6 T. Calvet, M. Labrador, E. Tauler, E. Estop, M.A. Cuevas-Diarte and Y. Haget, *Thermochim. Acta*, 147 (1989) 273.
- 7 D. Mondieig, Thèse de l'Université Bordeaux I, 1988.
- 8 D. Mondieig, M.A. Cuevas-Diarte and Y. Haget, *J. Therm. Anal.*, 35 (1990) 7.
- 9 H. Rheinboldt, M. Perrier, E. Giesbrecht, A. Levy, M.A. Cecchini and H. Viera de Campos, *Quim. (Barcelona)*, 3 (1951) 29.
- 10 R. Courchinoux, N.B. Chanh, Y. Haget, E. Tauler and M.A. Cuevas-Diarte, *Thermochim. Acta*, 128 (1988) 45.
- 11 R. Courchinoux, N.B. Chanh, Y. Haget, T. Calvet, E. Estop and M.A. Cuevas-Diarte, *J. Chim. Phys.*, 86 (3) (1989) 561.
- 12 F.H. Herbstein, *Acta Crystallogr.*, 18 (1965) 997.
- 13 G. Gafner and F.H. Herbstein, *Mol. Phys.*, 1 (1959) 412.